Essential Readings in Light Metals: Electrode Technology for Aluminum Production.
Edited by Alan Tomsett and John Johnson.

From ***Light Metals 1984***, J.P. McGeer, Editor

FACTORS IN THE DESIGN OF REDUCTION CELL ANODES

D. G. Brooks and V. L. Bullough

Reduction Laboratory
Reynolds Metals Company
P. O. Box 1200
Sheffield, AL 35660 USA

Introduction

As the aluminum industry tends toward the large, multi-stubbed anodes for low current density operation, the design factors affecting the mechanical and thermal stresses acting on an in-service anode become increasingly important. The design should be such that the resulting stresses are well removed from the mechanical limits of the carbon while, simultaneously, providing for minimum stub-to-carbon contact drops.

Anode electrical connections are secured by placing the steel stub(s) in the anode stub hole(s) and pouring molten cast iron in the annular spacing. During cell operation, the anode carbon can be mechanically stressed by the strain imposed through the stub hole by the thermal expansion of the stub and cast iron. Thermal stresses occur when an anode block, at ambient temperature, is set in the reduction cell with bath temperatures on the order of 950°C. When these stresses exceed the mechanical limits of the carbon, anode failure or cracking can occur.

Experiments were performed to: (1) Verify the reliability of carbon strain calculations through a stub hole brought on by the expansion of the steel stub and cast iron; (2) Determine the strain or "tightness of fit" necessary to minimize the stub-to-carbon contact resistance; and (3) Determine, at least qualitatively, the degree of thermal stress exerted on an operating anode.

Calculation of Stub Hole Strain

A simple series of calculations was used to determine the degree of carbon strain exerted across a stub hole based upon the elementary principles of thermal expansion. The calculations assume that strain can be estimated by the following relationship

$$\varepsilon = (E_n - d)/\ell_o \ , \ E_n \geq d \qquad (1)$$

where

ε = Strain across stub hole; inches/inch

E_n = Net expansion within stub hole including effects of stub, cast iron and carbon; inches

d = Air gap between cast iron and carbon surfaces at ambient temperature; inches

ℓ_o = Stub hole diameter with free expansion, inches

The air gap arises because of the cast iron and stub shrinkage after casting.

The expansions and air gap can be calculated from the coefficients of thermal expansion (CTE), cast iron shrinkage data and casting and operation temperatures.

Procedure

Deflections in and around a stub hole were determined experimentally and analyzed in much the same fashion as that reported by Peterson(1). A double-stubbed prebake anode measuring 31" x 52" and a steel yoke were prepared for testing. Provision was made for measuring deflections by threading 3/4" carbon steel rods at selected positions in the top of the block. Slat steel was welded to the rods to provide convenient measuring points. Deflections were measured with dial calipers (0.001"). Thermocouples were installed at strategic locations within the block and yoke for obtaining temperature gradients and distribution. Inconel tubing was placed within the stub holes prior to casting to provide thermocouple wells for measuring stub hole temperatures. See Figure 1 for a schematic representation.

Measurements of deflection were performed while using a baking pit of an open top, ring carbon baking furnace as a heating source. Here, the vertical temperature gradients could simulate, in some way, those gradients that would be expected in a reduction cell. Temperatures were recorded with a data logger.

Deflections were measured and recorded manually at regular time intervals. The temperature distribution across the slat steel was also recorded to provide for expansion corrections, which was negligible in most cases. Deflections were measured at three vertical points and extrapolated to the carbon surface. The experiment continued for approximately 72 hours.

Upon completion of this experiment, the assembly was pulled from the baking pit, cooled and prepared for additional testing while in service in a reduction cell. The thermocouples were left intact and the steel works

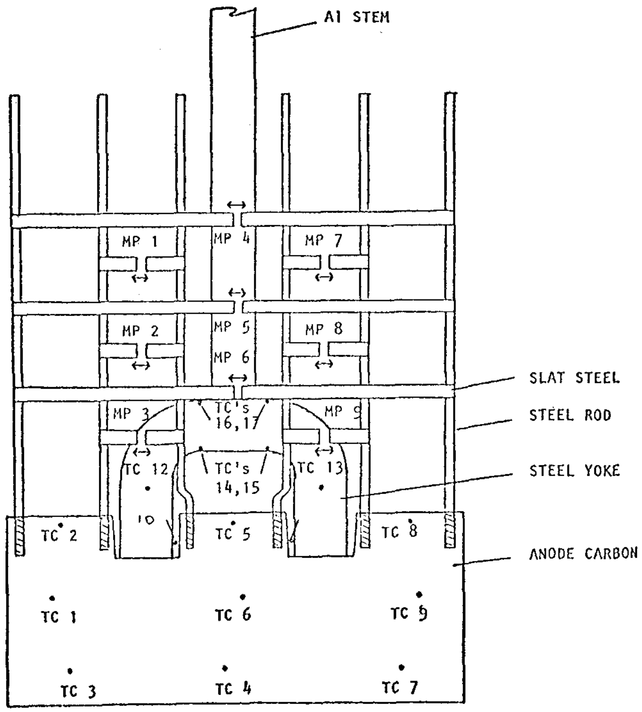

Figure 1 - Experimental Set-Up for Measuring Temperatures And Expansions of Anode/Yoke Assembly.

used in measuring deflections were removed, with the exception of about 8" of steel rodding on each side of each stub hole. These points were used as voltage probes for measuring stem-to-carbon voltage drops.

The prepared assembly was then set in a reduction cell operating at 152 kA as a corner anode according to the normal setting pattern and procedures. Both temperature and voltage data were recorded with a data logger. Refer to Figure 2. Data were obtained for the first 45 hours of service life.

Results

Deflection Experiment Results

The deflection experiments were carried out to determine the amount of strain being imposed on the carbon from the thermal expansion of the yoke steel, and to provide an experimental point to verify the reliability of calculations. An attempt was also made to measure experimentally the bowing of an anode as reported by other investigators(1). The bowing action is believed to result in an increased interference fit (strain) through the stub holes.

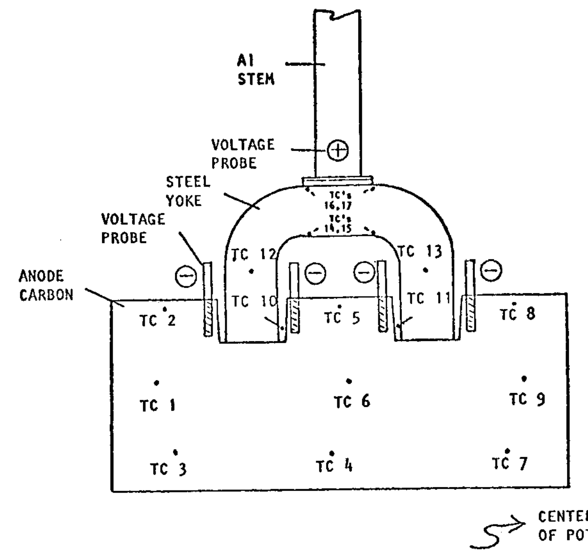

Figure 2 - Experimental Set-Up for Determining Thermal Gradients and Contact Voltge Drops.

Substantial scatter was found in the deflection measurements, as expected. A large number of readings were obtained to partly compensate for this scatter.

Block expansion versus mean block temperature is demonstrated in Figure 3. The scatter in the experimental points is apparent; however, the experimental data are in good agreement with the predicted expansion as determined from the coefficient of thermal expansion (CTE). The mean block temperature was obtained by two-dimensional integration over the height and length of the block. CTE values were determined experimentally with a dilatometer furnace.

If significant bowing of the anode occurs, it would be most apparent in the block deflection measurement of Figure 3, resulting in the experimental deflection being less than the predicted expansion. The bowing effect was not observed in this case, although a slight effect may not have been detectable because of the data scatter.

Expansion effects across a stub hole are shown in Figures 4 and 5. When the temperature first begins to rise, the expansion is expected to follow that of carbon alone. This is because of the air gap that is initially present in an anode/yoke assembly that is adjoined with cast iron. The air gap provides a buffer for free expansion of the steel stub and cast iron, and throughout this expansion the carbon is not stressed.

The thermal expansion coefficient of steel is greater than that of carbon, causing the connection to eventually tighten. Upon tightening, the stub hole would be expected to expand at the rate of the yoke steel, cast iron and residual carbon between reference points, all combined.

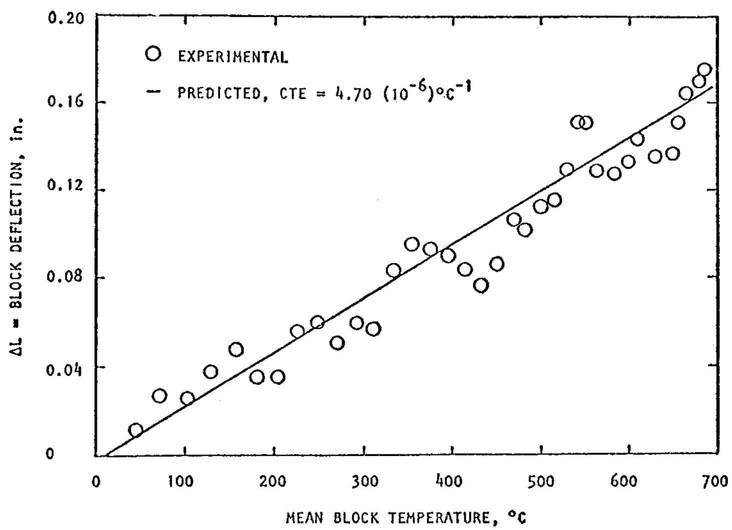

Figure 3 - Linear Block Deflection as Function of Mean Block Temperature.

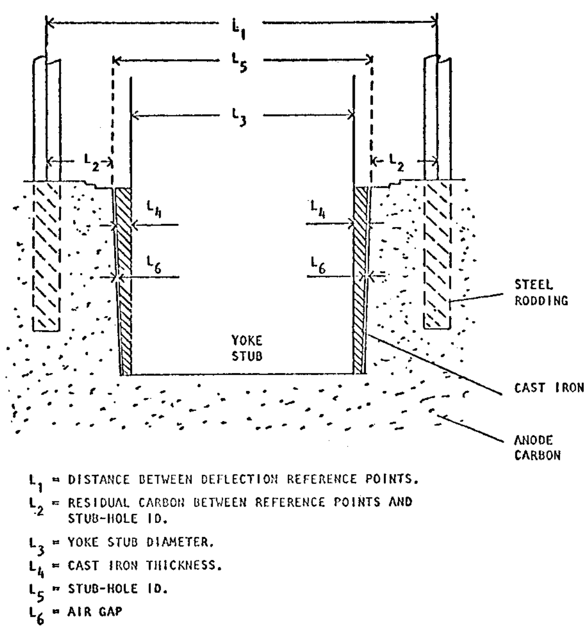

Figure 4 - Schematic Representation of Anode/Stub Electrical Connection.

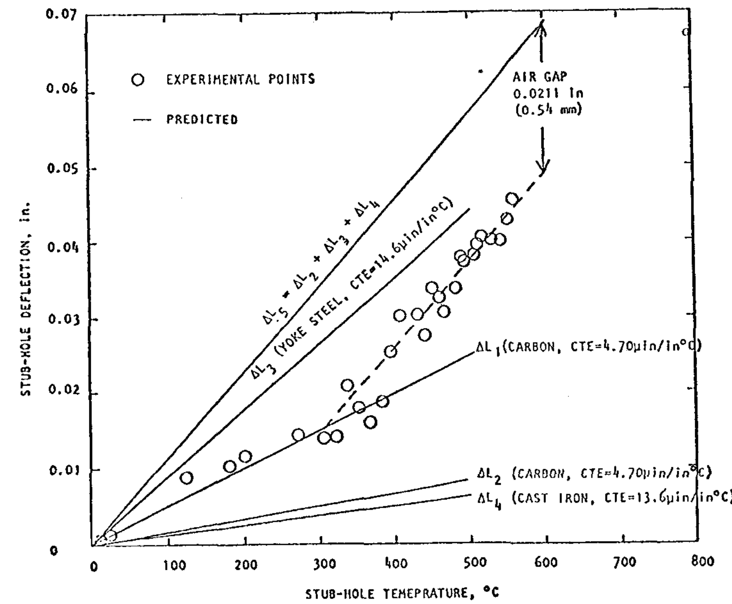

Figure 5 - Experimental and Predicted Expansions Within Stub Hole. Refer to Figure 4 for Schematic Representation.

The predicted effects, along with experimental measurements, are shown in Figure 5. Initially, before the stub/carbon connection tightens, the stub hole is expected to expand at a rate designated by ΔL_1, which is the expansion of anode carbon between reference points. The experimental points follow this expansion until temperatures reach about 300-350°C.

Predicted expansions of the residual carbon, steel stub and cast iron are given by ΔL_2, ΔL_3 and ΔL_4, respectively. The additive effect is also given, ΔL_5. Above 300-350°C, the experimental data show expansion at very nearly the same rate as ΔL_5 which is indicative that the stub/carbon connection has tightened and the carbon is being stressed.

Had there been no air gap initially present, the measured expansions would have followed the line given by ΔL_5 from the beginning. Therefore, a measure of the air gap can be obtained from the difference of the intercepts between the line given by ΔL_5 and the parallel experimental expansion. Forcing the rate of expansion (slope) of the experimental deflection to be parallel with ΔL_5, and performing a least-squares fit on the intercept alone, yields an air gap of 0.0211" (0.54 mm), which is in excellent agreement to that predicted from casting temperatures, anode design and cast iron shrinkage data.

These results demonstrate that strain loads through a stub hole can be estimated with a high degree of reliability from simple calculations based on the elementary principles of thermal expansion together with casting and operational temperature data.

Cell Operation Results

The information obtained on an in-service anode is useful in determining the temperatures at which the stub/carbon connection resistance is minimized. This temperature is representative of some strain load on the carbon and can be used for sizing an optimum, or near optimum, stub hole diameter to achieve minimum voltage drops at an acceptable carbon stress.

The operating thermal gradients can also be used to analyze, at least qualitatively, the thermal stresses imposed on an anode.

Figure 6 represents the decrease in contact voltage drop with increasing stub hole temperature as the anode service life progresses. Initially, the voltage drop increases rapidly as the anode begins to draw current. This is followed by a moderate rate of decrease in resistance as the yoke steel and connections are heated. After about 24 hours, the voltage drop becomes relatively constant, while stub temperatures continue to rise slowly. This is indicative that the decrease in contact resistance brought about by carbon strain has been fully realized; further stress through the stub hole is of little or no benefit and increases the risk of breakage.

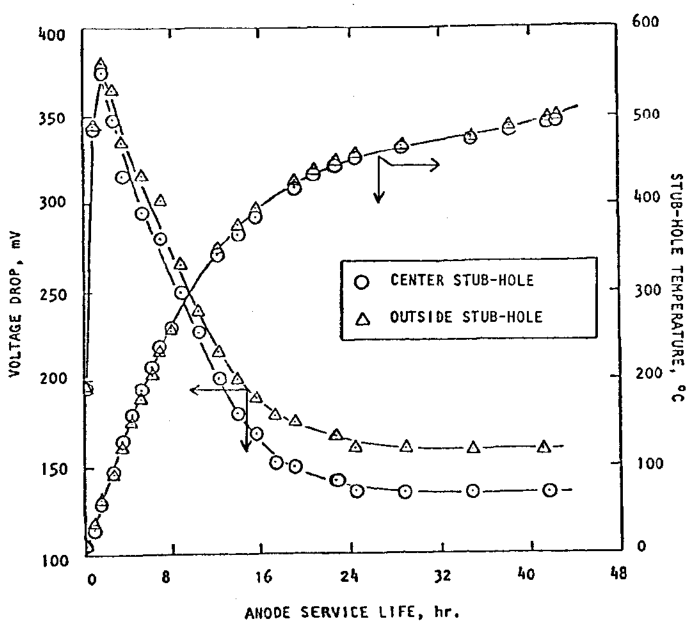

Figure 6 - Contact Voltage Drop and Temperture Response Versus Anode Service Life.

The service life of a low density anode is on the order of 20 days, during which time the carbon is consumed and the stub/carbon connections continue to be lowered closer to the bath. Thus, stub temperatures will continue to increase, possibly to as much as 700°C resulting in considerably more stress on the carbon. The stub holes should be appropriately sized so that the mechanical stresses exerted on the carbon result in minimum contact voltage drops, yet are sufficiently removed from the stress limit of the carbon.

The analysis of thermal stress requires a knowledge of the temperature gradients developing through the stressed body. These gradients have been measured experimentally and are depicted in Figures 7 and 8. An important point to note is that the overall gradient is not important, but rather the temperature profile through the block.

A rigorous analysis of thermal stresses in a reduction cell anode is very complicated. To simplify the analysis, the theory of thermal stresses in beams is used. While this is an oversimplification of the actual system, it can be used to analyze, at least qualitatively, for the relative magnitudes of thermal stress. In such a case the distribution of thermal stress is given by(2)

$$\sigma_T = \frac{-\alpha TE}{1-\nu} + \frac{E\alpha}{2b(1-\nu)}\int_{-b}^{b} T dy + \frac{3E\alpha y}{2b^3(1-\nu)}\int_{-b}^{b} Ty dy \qquad (2)$$

where

σ_T = Thermal stress
α = Coefficient of thermal expansion
E = Modulus of elasticity
ν = Poisson's ratio
2b = Anode thickness (height)
T = Temperature
y = Depth coordinate through anode (center @ y = o)

Equation 2 can be expressed in dimensionless form as

$$\sigma^* = \frac{\sigma(1-\nu)}{E\alpha T_o} = -T^* + 1/2\int_{-1}^{1} T^* dy^* + \frac{3y^*}{2}\int_{-1}^{1} T^* y^* dy^* \qquad (3)$$

where

To = Initial temperature
T^* = T/To
y^* = y/b
σ^* = Dimensionless thermal stress

Equation 3 is a measure of the relative thermal stress as a function of position (depth) through the anode block. This equation has been used in conjunction with the thermal gradients to obtain relative values of thermal stress, and the results are given in Figure 9, where maximum dimensionless thermal stress (tensile) is plotted as a function of service

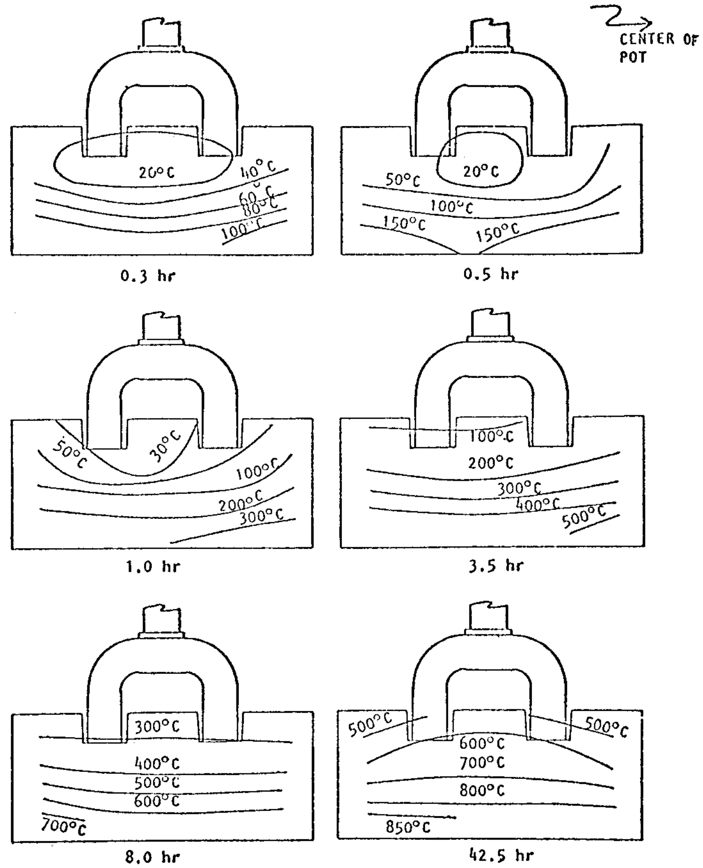

Figure 7 - Temperature Isotherms in an Operating Anode As a Function of Service Life.

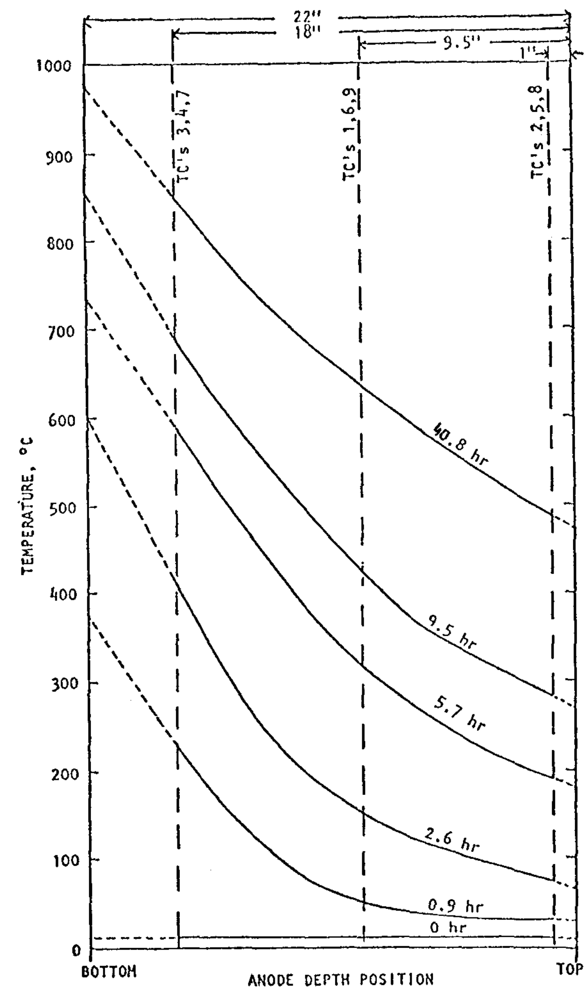

Figure 8 - Temperature/Depth Profiles in an Operating Anode as a Function of Anode Service Life.

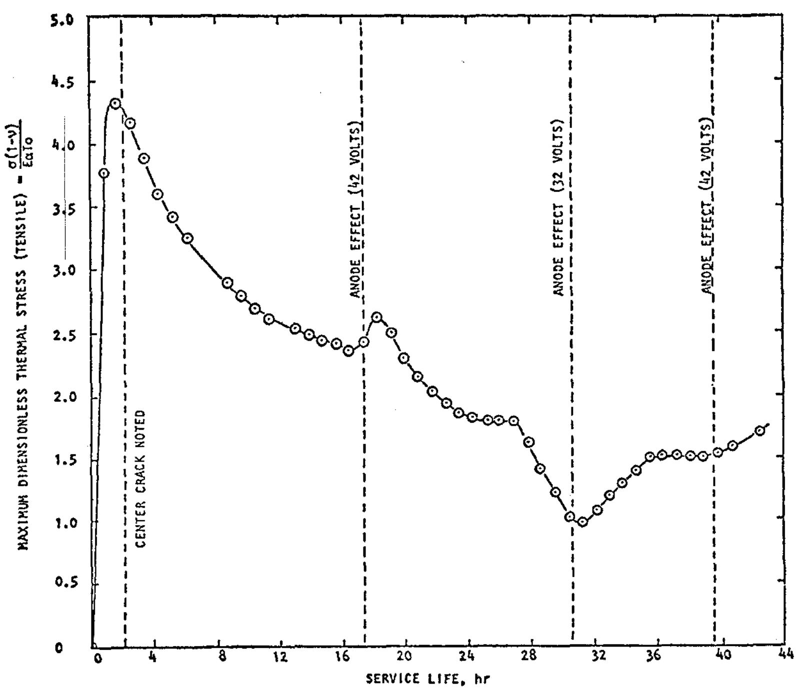

Figure 9 - Relative Magnitudes of Thermal Stress Exerted on an Operating Anode as a Function of Anode Service Life.

life. These results demonstrate that the most severe thermal stress occurs within the first few hours of operation. This is the thermal shock effect, and is expected when a cold anode is first set in hot bath.

It is interesting to note that the anode used in this test cracked between stubs shortly after set. This crack was first noted at 2 hours 8 minutes after set, but could have occurred a short time before. This is a period of high thermal stress, and suggests that thermal stress is a major factor resulting in early anode breakage, particularly the center cracks between stubs.

The results of Figure 9 also hint that anode effects can increase thermal stress, although it is not conclusive that this is so. In every case, the thermal stress tends to rise following an anode effect, but the magnitude does not appear to be significant when compared with the initial thermal shock. Also, the continual rise in thermal stress over a period of 6 hours, as seen following the second anode effect, is difficult to rationalize since an anode effect lasts for only a brief period of time, and the heat generated is expected to dissipate quickly.

An anode that does not crack early in service is not likely to fail later from thermal stress alone. However, some degree of thermal stress is always present and could be a contributing factor when coupled with the mechanical stresses that may occur later in the service life as the yoke and the stubs continue to increase in temperature.

Discussion

Mechanical Effects

The decrease in contact drop with anode service life, as shown in Figure 6, could be attributed partly to a temperature effect. Laboratory results demonstrate that both temperature and contact pressure affect contact resistance. However, as demonstrated in Figure 10, the effect of increasing either temperature or contact pressure is minimal once the contact pressure becomes sufficient; a moderate pressure of 150 psi in this case. Thus, the minimum voltage drops attained in Figure 6 is believed to result from obtaining a sufficient contact pressure, i.e., a sufficient carbon strain.

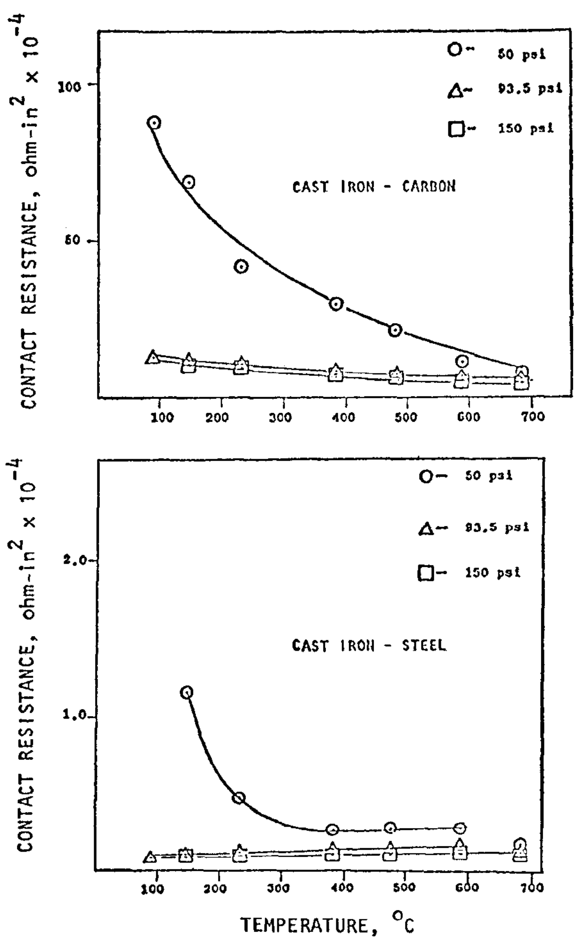

Figure 10 - Contact Resistance as a Function of Temperature and Pressure.

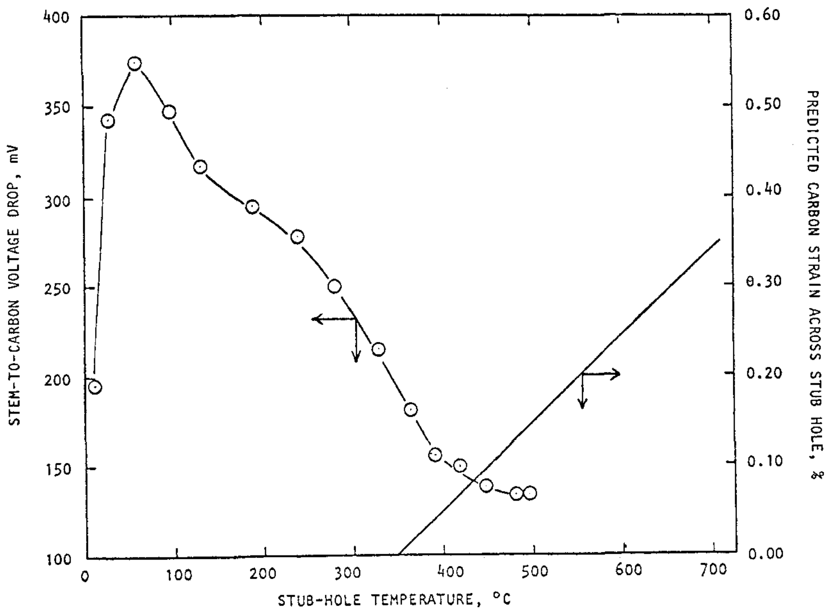

Figure 11 - Voltage Drop and Strain Load Through Stub Hole As a Function of Stub-Hole Temperature.

It is demonstrated in Figure 6 that, for the particular design in this test, stub hole temperatures of 450°C and above yield minimum contact drops. These temperatures also correspond to certain strain loads through the stub hole. Both effects are presented in Figure 11. The contact resistances are minimum at strains of greater than 0.10%.

How much carbon strain is desired is a compromise. It is possible to design for a carbon strain that is just sufficient to minimize contact voltage drops; but this leaves little room for error or minor modifications in rodding or potroom practices, and risks the possibility that the resulting contact drops will be greater than desired. It is better to design for a moderate carbon strain such that minor changes in operations would always provide for minimum contact resistance while remaining below the mechanical limits of the carbon.

Based on this study, it is believed that a carbon strain of 0.20% at 600°C would result in a near optimum design. A strain of 0.20% is well removed from the strain limit of most carbon bodies, so that temperatures above 600°C (up to about 700°C) would not result in breakage. Furthermore, a strain moderately below 0.20% would still provide for low contact resistance; thus, obtaining low voltage drops early in the anode service life.

Using these design criteria, the desired stub hole diameter can be calculated. The important variables are stub diameter, CTE of the stub and CTE of the anode carbon. A set of design charts has been prepared and is given by Figure 12. These charts cover the range of variables normally encountered. Thus, if the above variables are known, a near optimum stub hole diameter can be estimated.

It should be pointed out that these charts are valid only for the anode/stub assemblies adjoined with cast iron. Also, the amount of preheat on the stubs prior to casting is considered mild, i.e., sufficient for removing moisture.

These design charts should provide a logical starting point when designing a new anode/stub assembly, either as a wholly new cell design or as a retrofit of existing cells.

Thermal Effects

Practical means of reducing thermal stress are not readily apparent. Invariably, a cold anode is going to be thermally stressed when placed in hot bath. The degree of thermal stress can be influenced by the mechanical and thermal properties of the carbon.

The effect of carbon properties has been discussed previously(3). The thermal stress resistance of carbon can be enhanced by increasing the parameter:

$$TSR = \frac{FS \times k}{E \times \alpha} \qquad (4)$$

where

TSR = Thermal stress resistance
FS = Flexural strength
k = Thermal conductivity
E = Modulus of elasticity
α = Coefficient of thermal expansion

Therefore, a change in carbon processing to increase FS, k and/or decrease E, α will result in a more stress resistant anode.

Two different anode types have been tested in a reduction cell operating at 152 kA. The properties of these anode regarding thermal stress resistance are given in Table I.

Table I. Anode Carbon Properties Pertaining to Thermal Stress

Anode	FS, psi	k, W/m°C	$E \times 10^5$ psi	$\alpha \times 10^{-6}$ μin/in°C	$TSR \times 10^3$ W/m
Type A	1090	5.06	3.31	4.56	3.65
Type B	1578	5.70	3.16	4.70	6.02

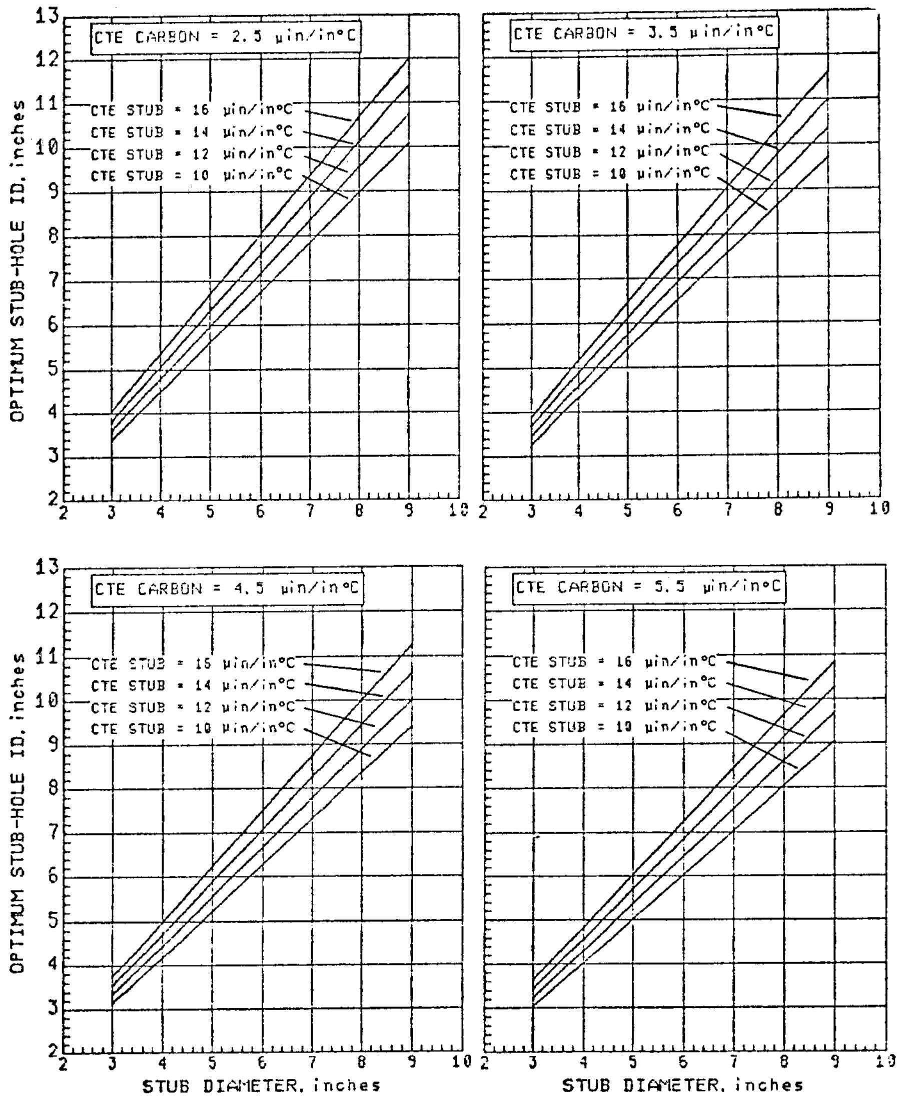

Figure 12 - Design Charts for Sizing Optimum Stub-Hole ID With Cast Iron Connections.

The results from cell operations indicate that the Type B anode is a superior anode to Type A regarding resistance to cracking. Whether or not this is directly attributal to improved thermal stress resistance is not known in that the increased flexural strength would also result in improved resistance to mechanical stress.

Conclusion

Minimum stem-to-carbon contact resistance in an operating anode are obtained at a moderate strain load of greater than or equal to 0.10%. Increased strain offers little benefit while increasing the risk of anode breakage. Design and operational data provide a basis for estimating the strain imposed across a stub hole, allowing for the sizing of a near optimum stub hole diameter.

Thermal stresses are most critical within the first few hours of anode service, but some degree of thermal stress is always present.

Acknowledgement

The authors would like to acknowledge the contribution of C. J. McMinn of the Reynolds Metals Company Reduction Laboratory regarding the information of metal/carbon electrical resistances.

References

1. Peterson, R. W., "Studies of Stub to Carbon Voltage," Light Metals 1978, p. 367.

2. Boley, B. A. and J. H. Weiner, Theory of Thermal Stresses, John Wiley & Sons, Inc., 1960.

3. Brown, J. A. and P. J. Rhedey, "Characterization of Prebaked Anode Carbon by Mechanical and Thermal Properties," Light Metals 1975, p. 263.